

# FSTPI Fed Induction Motor Emulating the SSTPI Operation by Using DTC method

A.V.G.A.Marthanda<sup>1</sup> Dr. G.V.Marutheswar<sup>2</sup>

<sup>1</sup>Associate professor, Dept. of EEE Laki Reddy college of Engineering Mylavaram Krishna Dist., Andhra Pradesh, India

<sup>2</sup>Professor, Department Of Electrical & Electronics Engineering, S.V. University College of Engineering Tirupathi, Andhra Pradesh, India

**Abstract:** This paper describes a combination of direct torque control (DTC) and space vector modulation (SVM) for an adjustable speed sensor less induction motor (IM) drive. In this paper we introduced a new strategy i.e., the induction motor drives fed by a four switch inverter emulate the operation of the conventional six switch operation. Therefore, a suitable combination of the four unbalanced voltage vectors intrinsically generated by the FSTPI, leading to the synthesis of the six balanced voltage vectors of the SSTPI. Simulation results have revealed that, the proposed DTC strategy with SVM modulation, FSTPI-fed IM drives exhibit interesting performance.

**Index Terms**—Direct torque control (DTC), Space vector modulation (SVM), SSTPI, FSTPI-fed IM drives.

## I. INTRODUCTION

Direct torque control (DTC) is a high-dynamic and high performance control technique for induction motor drives which has been developed in the last two decades as possible alternative to DC servo drives. In direct torque controlled adjustable speed drives, the motor flux and the electromagnetic torque are the reference quantities which are directly controlled by the applied inverter voltage vector. The main advantages of DTC are: fast torque and flux responses, no need for speed or position sensors and no requirements for coordinate transformation. In fact, it only needs to know the stator resistance and terminal quantities ( $v$  and  $i$ ) in order to perform the stator flux and torque estimations. Therefore, the DTC schemes have attracted many researchers to study and investigate for a long time.

The DTC using a multi-level inverter can produce more sets of space vectors to control torque and flux of a motor and gain smoother electromagnetic torque of the motor. However, the multi-level inverters need more power switch elements and cause more cost and complication to the whole system. By combining the advantages of matrix converters with the advantages of DTC schemes, it is possible to achieve fast torque and flux responses in a wide speed range. But the main drawback of the conventional DTC will make more serious electromagnetic torque ripple. As a result, the drive system fed by the matrix converter doesn't need any additional power switch elements and can attain the same performance as the multi-level inverter. According to the properties of a matrix converter, there are three different voltage vectors on each space vector location. By suitably selecting the space vector, the current deviations and the torque ripple of the motor can be effectively reduced. This paper proposes to select the most appropriate voltage vector with respect to the error of the torque. The standard look-up table for direct torque control by matrix converters is improved in order to include the small, medium and large voltage vectors of Matrix Converters. With the new look-up table and new hysteresis comparator with seven levels output the system will

differentiate between small, medium and large torque errors and consequently reduce the electromagnetic torque ripple and output current THD. Simulation results demonstrate the effectiveness of the proposed scheme.

This paper proposes a new DTC strategy dedicated to FSTPI fed IM drives. It is based on the emulation of the SSTPI operation thanks to the synthesis of an appropriate vector selection table, which is addressed by hysteresis controllers. The resulting simplicity of the implementation scheme makes the strategy very attractive in many applications, such as the automotive one.

## II. DTC OF FSTPI-FED IM DRIVES: BACKGROUND

### A. DTC Basis:

DTC strategies allow a direct control of the motor variables through an appropriate selection of the inverter control signals, in order to fulfill the requirements as whether the stator flux and torque need to be increased, decreased, or maintained. These decisions are achieved according to the output  $c\phi$  of the flux hysteresis controller, the output  $c\tau$  of the torque hysteresis controller, and the angular displacement  $\theta_s$  of the stator flux vector  $\Phi_s$  in the Clarke ( $\alpha\beta$ ) plane. The dynamic of  $\Phi_s$  is governed by the stator voltage equation expressed in the stationary reference frame, as follows.

$$\frac{d}{dt} \Phi_s = V_s - r_s I_s \quad (1)$$

where  $V_s$ ,  $I_s$ , and  $r_s$  are the stator voltage vector, current vector, and resistance, respectively. Neglecting the voltage drop  $r_s I_s$  across the stator resistance, and taking into account that the voltage vector is constant in each sampling period  $T_s$ , the variation of the stator flux vector turns to be proportional to the applied voltage vector. Maintaining the stator flux constant, the variation of the electromagnetic torque  $T_{em}$  depends on the direction of the applied voltage vector, such that

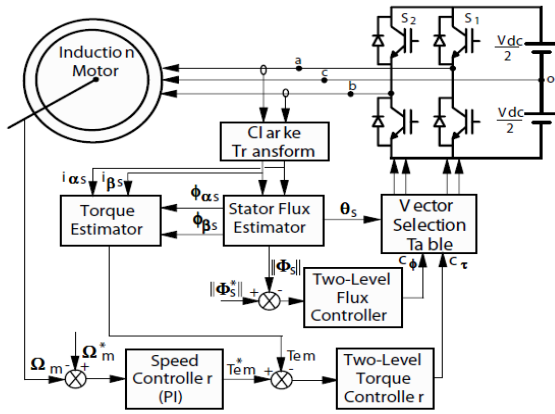


Fig 1. Implementation scheme of the DTC strategy dedicated to FSTPI-fedIM drives.

$$T_{em} = N_p \frac{M}{l_r l_s - M^2} \|\Phi_s\| \|\Phi_r^s\| \sin \delta \quad (2)$$

where  $\Phi_{sr}$  is the rotor flux vector referred to the stator,  $\delta$  is the angular shift between the stator and rotor fluxes,  $N_p$  is the pole pair number, and  $l_s$ ,  $l_r$ , and  $M$  are the stator self-inductance, the rotor self-inductance, and the mutual inductance, respectively. The implementation scheme of the DTC strategy dedicated to a FSTPI-fed IM, shown in Fig. 1, has the same layout as the one of the basic DTC strategy initially proposed in except that

- The SSTPI inverter is reconfigured to a FSTPI. Such are configuration is carried out by adding to the former three extra TRIACs with three fast acting fuses .
- The three-level hysteresis controller in the torque loop is substituted by a two-level hysteresis controller. As will be depicted in Section III, this substitution is motivated by the fact that no zero voltage vector is involved in the proposed DTC scheme

TABLE I SWITCHING STATES, STATOR PHASE VOLTAGES, THEIR Clarke COMPONENTS AND CORRESPONDING VOLTAGE VECTORS

(S <sub>1</sub> S <sub>2</sub> )	V <sub>as</sub>	V <sub>bs</sub>	V <sub>cs</sub>	V <sub>αs</sub>	V <sub>βs</sub>	V <sub>i</sub>
(0 0)	$-\frac{V_{dc}}{6}$	$-\frac{V_{dc}}{6}$	$\frac{V_{dc}}{3}$	$-\frac{V_{dc}}{2\sqrt{6}}$	$-\frac{V_{dc}}{2\sqrt{2}}$	V <sub>1</sub>
(1 0)	$\frac{V_{dc}}{2}$	$-\frac{V_{dc}}{2}$	0	$\frac{3V_{dc}}{2\sqrt{6}}$	$-\frac{V_{dc}}{2\sqrt{2}}$	V <sub>2</sub>
(1 1)	$\frac{V_{dc}}{6}$	$\frac{V_{dc}}{6}$	$-\frac{V_{dc}}{3}$	$\frac{V_{dc}}{2\sqrt{6}}$	$\frac{V_{dc}}{2\sqrt{2}}$	V <sub>3</sub>
(0 1)	$-\frac{V_{dc}}{2}$	$\frac{V_{dc}}{2}$	0	$-\frac{3V_{dc}}{2\sqrt{6}}$	$\frac{V_{dc}}{2\sqrt{2}}$	V <sub>4</sub>

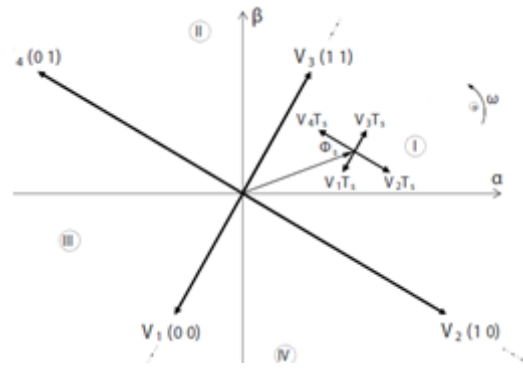


Fig 2. Unbalanced active voltage vectors generated by the FSTPI

A . Intrinsic Voltage Vectors of the FSTPI

The FSTPI topology consists of a two-leg inverter as illustrated in Fig. 1. Two among the three phases of the motor are connected to the FSTPI legs, while the third one is connected to the middle point of the dc-bus voltage. Let us assume that the states of the four insulated-gate bipolar transistors (IGBTs) of the FSTPI are denoted by the binary variables S<sub>1</sub> to S<sub>4</sub>, where the binary “1” corresponds to an ON state and the binary “0” indicates an OFF state. The IM stator voltages are expressed in terms of the states (S<sub>1</sub> and S<sub>2</sub>) of the upper IGBTs, as follows:

$$\begin{bmatrix} V_{as} \\ V_{bs} \\ V_{cs} \end{bmatrix} = \frac{V_{dc}}{6} \begin{bmatrix} 4 & -2 & -1 \\ -2 & 4 & -1 \\ -2 & -2 & 2 \end{bmatrix} \begin{bmatrix} S_1 \\ S_2 \\ 1 \end{bmatrix} \quad (3)$$

The Clarke transform applied to the stator voltages yields:

$$\begin{bmatrix} V_{\alpha s} \\ V_{\beta s} \end{bmatrix} = \sqrt{\frac{2}{3}} \begin{bmatrix} 1 & -\frac{1}{2} & -\frac{1}{2} \\ 0 & \frac{\sqrt{3}}{2} & -\frac{\sqrt{3}}{2} \end{bmatrix} \begin{bmatrix} V_{as} \\ V_{bs} \\ V_{cs} \end{bmatrix} \quad (4)$$

Four combinations of the states of the upper IGBTs are characterized by four active voltage vectors (V<sub>1</sub> to V<sub>4</sub>) in the  $\alpha\beta$  plane, which are given in Table I. Fig. 2 shows the four active voltage vectors represented in the  $\alpha\beta$  plane. These vectors have unbalanced amplitudes and are shifted by an angle of  $\pi/2$ . Indeed, vectors V<sub>1</sub> and V<sub>3</sub> have

TABLE II VECTOR SELECTION TABLE OF THE BASIC DTC STRATEGY

c <sub>φ</sub>	+1	+1	-1	-1
c <sub>τ</sub>	+1	-1	+1	-1
Sector I	V <sub>3</sub>	V <sub>2</sub>	V <sub>4</sub>	V <sub>1</sub>
Sector II	V <sub>4</sub>	V <sub>3</sub>	V <sub>1</sub>	V <sub>2</sub>
Sector III	V <sub>1</sub>	V <sub>4</sub>	V <sub>2</sub>	V <sub>3</sub>
Sector IV	V <sub>2</sub>	V <sub>1</sub>	V <sub>3</sub>	V <sub>4</sub>

an amplitude of  $V_{dc}/\sqrt{6}$ , while vectors V<sub>2</sub> and V<sub>4</sub> have an amplitude of  $V_{dc}/\sqrt{2}$ .

**B.Limitations of the Basic DTC of a FSTPI-Fed IM**

The basic DTC of an IM fed by the FSTPI is based on the subdivision of the  $\alpha\beta$  plane into four sectors [17], limited by the four active voltage vectors as shown in Fig. 2. The vector selection table corresponding to the basic strategy is presented in Table II. Accounting for the symmetry of the four sectors, the following analysis of the torque and flux variations, will be limited to sector I, considering two cases:1) the initial stator flux vector  $\Phi_{s1}$  is held by vector **V2** ;2) the initial stator flux vector  $\Phi_{s1}$  is held by vector **V3** .Equation (1) could be rewritten as follows:

$$\Phi_{s2}^1 = \Phi_{s1} + (V_i - r_s I_s) T_s \tag{5}$$

where  $V_i$  ( $1 \leq i \leq 4$ ) is the voltage vector generated by the FSTPI .Fig. 3 shows different pharos diagrams of (5), considering both cases previously cited with four scenarios selected from the vector selection table, for each. One can notice the following remarks which deal with the torque dynamic.

- The application of voltage vectors **V1** or **V3** leads to a low torque dynamic if:  $\Phi_{s1}$  is close to vector **V2** due to the low amplitude of **V1** and **V3** [see Fig. 3(a1) and (a3)];b)  $\Phi_{s1}$  is close to vector **V3** due to the low angular shift of the flux vector [see Fig. 3(b1) and (b3)]. It is to be noted that the torque command  $c\tau$  of the control combinations ( $c\varphi = -1, c\tau = +1$ ) corresponding to sector II and ( $c\varphi = +1, c\tau = +1$ ) corresponding to sector I could not be achieved by the application of vectors **V1** and **V3** , respectively.
- The application of voltage vectors **V2** or **V4** leads to a low torque dynamic if  $\Phi_{s1}$  is close to vector **V2** due to the low angular shift of the flux vector [see Fig. 3(a2)and (a4)]. One can notice One can notice that the control combinations ( $c\varphi = +1, c\tau = +1$ ) corresponding to sector IV and( $c\varphi = -1, c\tau = +1$ ) corresponding to sector I could not be achieved with the application of voltage vectors **V2**and **V4** , respectively.
- The application of voltage vectors **V2** or **V4** leads to a high torque dynamic if  $\Phi_{s1}$  is located near vector **V3** [see Fig. 3(b2) and (b4)]. Concerning the flux dynamic, one can notice the following.1) High flux variations leading to overshoots or under shoots outside the flux hysteresis band with :a) the application of voltage vectors **V1** or **V3** if  $\Phi_{s1}$  is close to vector **V3** [see Fig. 3(b1) and (b3)];

The application of voltage vectors **V2** or **V4** if  $\Phi_{s1}$  is close to vector **V2** [see Fig. 3(a2) and (a4)].2) The flux command  $c\varphi$  is not achieved with the application of: a) vector **V1** in sector IV corresponding to the control combination ( $c\varphi = +1, c\tau = -1$ ) as illustrated in Fig. 3(a1).Vector **V2** in sector I corresponding to the control combination( $c\varphi = +1, c\tau = -1$ ) as illustrated in Fig. 3(b2).Vector **V3** in sector I corresponding to the control

combination ( $c\varphi = +1, c\tau = +1$ ) as illustrated in Fig. 3(a3). Vector **V4** in sector II corresponding to the control combination ( $c\varphi = +1, c\tau = +1$ ) as illustrated inFig. 3(b4).From the previous analysis, one can clearly notice that the basic DTC strategy presents different limitations. These could be eradicated considering the introduced DTC strategy which will be developed in the following section.

**III. PROPOSED DTC STRATEGY**

**A. Approach to Generate Balanced Voltages by the FSTPI**

The proposed DTC strategy is based on the emulation of SSTPI operation by the FSTPI. This has been achieved through the generation of six balanced voltage vectors using the four intrinsic ones of the FSTPI. The generated vectors have the same amplitude and angular shift as those of the SSTPI. Basically, the active voltage vectors  $V_k$ , with  $1 \leq k \leq 6$ , yielded by the SSTPI have an amplitude  $V_k$  equal to  $2/3 V_{dc}$ , where  $V_{dc}$  is the dc-bus voltage. For the same value of  $V_{dc}$ , the voltage vectors  $V_i$  , with  $1 \leq i \leq 4$ , generated by the FSTPI, present unbalanced amplitudes  $V_i$  , such that:

$$\begin{cases} V_1 = V_3 = \frac{V_{dc}}{\sqrt{6}} = \frac{1}{2} V_k \\ V_2 = V_4 = \frac{V_{dc}}{\sqrt{2}} = \frac{\sqrt{3}}{2} V_k. \end{cases} \tag{6}$$

Therefore, a dual application of the voltage vector **V1** (respectively, **V3** ) of the FSTPI, leads to the generation of the voltage vector **V11** (respectively, **V33**), as shown in Fig. 4. It is to be noted that **V11** and **V33** are identical to two vectors among the six generated by the SSTPI. Now, let us call **Vij** the voltage vectors resulting from the sums of successive voltage vectors  $V_i$  and  $V_j$  , with  $1 \leq i \leq 4$  and  $1 \leq j \leq 4$ . As far as the angular shift between two successive voltage vectors is equal to  $\pi/2$ , the amplitude  $V_{ij}$  of vectors **Vij** can be expressed as follows:

$$V_{ij} = \sqrt{V_i^2 + V_j^2} = \sqrt{\frac{1}{6} + \frac{1}{2}} V_{dc} = \sqrt{\frac{2}{3}} V_{dc} = V_k. \tag{7}$$

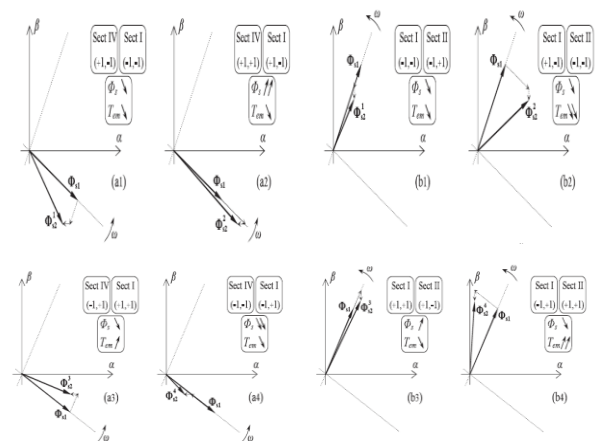


Fig. 3. Pharos diagrams describing the evolution of the stator flux vector in the case where it is located in the limits

of sector I. Legend: (a) initial flux vector  $\Phi_{s1}$  held by the voltage vector  $V_2$ , (b) initial flux vector  $\Phi_{s1}$  held by the voltage vector  $V_3$ .

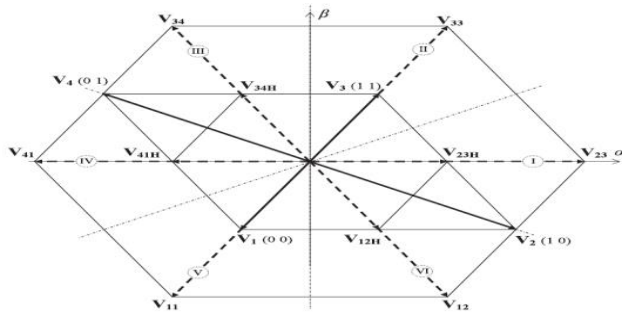


Fig. 4. Generation of the SSTPI active voltage vectors using the four unbalanced voltage ones of the FSTPI.

One can notice that the voltage vectors  $V_{ij}$  have the same amplitude as the ones generated by the SSTPI. Beyond the amplitude, the four generated vectors, named  $V_{12}, V_{23}, V_{34}$ , and  $V_{41}$ , as shown in Fig. 4, share the same phases with the four remaining active voltage vectors of the SSTPI. Table III summarizes the Clarke components of the six voltage vectors generated by the FSTPI considering the previously described approach

TABLE III Clarke COMPONENTS OF THE GENERATED VOLTAGE VECTORS

$V_{ij}$	$V_{23}$	$V_{33}$	$V_{34}$	$V_{41}$	$V_{11}$	$V_{12}$
$V_{\alpha s}$	$\sqrt{\frac{2}{3}}V_{dc}$	$\frac{V_{dc}}{\sqrt{6}}$	$-\frac{V_{dc}}{\sqrt{6}}$	$-\sqrt{\frac{2}{3}}V_{dc}$	$-\frac{V_{dc}}{\sqrt{6}}$	$\frac{V_{dc}}{\sqrt{6}}$
$V_{\beta s}$	0	$\frac{V_{dc}}{\sqrt{2}}$	$\frac{V_{dc}}{\sqrt{2}}$	0	$-\frac{V_{dc}}{\sqrt{2}}$	$-\frac{V_{dc}}{\sqrt{2}}$

Following the generation of six balanced active voltage vectors ( $V_{23}, V_{33}, V_{34}, V_{41}, V_{11}$ , and  $V_{12}$ ), the  $\alpha\beta$  plane turns to be subdivided into six symmetric sectors as illustrated in Fig. 4. Moreover, zero voltage vectors can be achieved through the application of two opposite intrinsic ones. The previously described approach represents a great control benefit so far as several DTC strategies implemented in SSTPI fed IM drives could be applied to FSTPI-fed IM ones.

A. Vector Selection Table of the Proposed DTC Strategy

The proposed DTC strategy is inspired from the earlier one introduced by Takahashi. For the sake of reduction of the switching frequency as well as the torque ripple, the control combinations ( $c_\phi = \cdot 1, c_\tau = 0$ ) are omitted using a two-level hysteresis controller in the torque loop. The synthesis of the vector selection table of the proposed DTC strategy is based on the approach described in the previous paragraph. Reaching this advanced step, one can wonder: how the control combinations ( $c_\phi = \cdot 1, c_\tau = \cdot 1$ ) could be

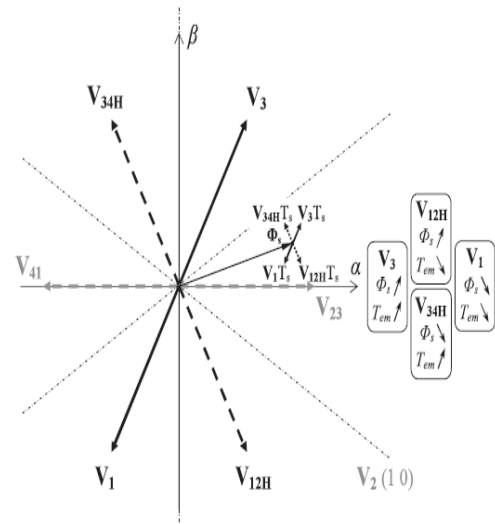


Fig. 5. Applied voltage vectors in the case where  $\Phi_{s1}$  is located in sector I.

Achieved applying the generated balanced voltage vectors. To answer this question, the following approach has been adopted. The application of  $V_1$  (respectively,  $V_3$ ) during two successive sampling periods  $2T_s$  allows the generation of  $V_{11}$  (respectively,  $V_{33}$ ). The application of two consecutive voltage vectors  $V_i$  and  $V_j$  during two successive sampling periods leads to the generation of  $V_{ij}$ . As a result, the equivalent voltage vectors per sampling period  $s$  generated by the FSTPI, considering the adopted approach, can be expressed as:

$$\begin{cases} V_{11H} = \frac{1}{2}V_{11} = V_1 \\ V_{33H} = \frac{1}{2}V_{33} = V_3 \\ V_{ijH} = \frac{1}{2}V_{ij} \end{cases} \quad (8)$$

where subscript  $H$  indicates the half of the corresponding voltage vector. In what follows, the synthesis of the vector selection table will be limited to sector I ( $-\pi/6 \leq \theta_s \leq \pi/6$ ). In this case and as shown in Fig. 5, the following voltage vectors are applied during a sampling period, according to the corresponding control combinations:

$$\begin{cases} V_3 & \text{for } (c_\phi = +1, c_\tau = +1) \\ V_{12H} & \text{for } (c_\phi = +1, c_\tau = -1) \\ V_{34H} & \text{for } (c_\phi = -1, c_\tau = +1) \\ V_1 & \text{for } (c_\phi = -1, c_\tau = -1). \end{cases}$$

In order to emulate the operation of the SSTPI, each control combination ( $c_\phi, c_\tau$ ) should be maintained during two sampling periods  $2T_s$ , which yields the application of:

$$\begin{cases} V_{33} & \text{for } (c_\phi = +1, c_\tau = +1) \Rightarrow V_3 \text{ then } V_3 \\ V_{12} & \text{for } (c_\phi = +1, c_\tau = -1) \Rightarrow V_1 \text{ then } V_2 \\ V_{34} & \text{for } (c_\phi = -1, c_\tau = +1) \Rightarrow V_3 \text{ then } V_4 \\ V_{11} & \text{for } (c_\phi = -1, c_\tau = -1) \Rightarrow V_1 \text{ then } V_1. \end{cases}$$

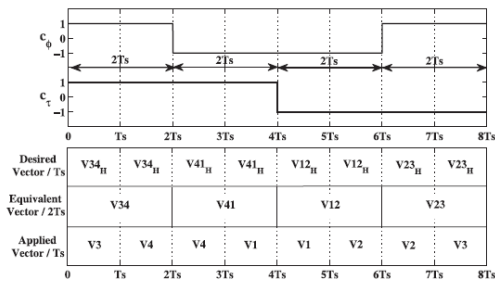


Fig. 6. Control combinations ( $c\phi$ ,  $c\tau$ ), desired voltage vectors per  $T_s$ , equivalent voltage vectors during  $2T_s$ , and applied voltage vectors per  $T_s$

TABLE IV DESIRED VECTOR SELECTION TABLE

$c_\phi$	+1	+1	-1	-1
$c_\tau$	+1	-1	+1	-1
Sector I	$V_3$	$V_{12H}$	$V_{34H}$	$V_1$
Sector II	$V_{34H}$	$V_{23H}$	$V_{41H}$	$V_{12H}$
Sector III	$V_{41H}$	$V_3$	$V_1$	$V_{23H}$
Sector IV	$V_1$	$V_{34H}$	$V_{12H}$	$V_3$
Sector V	$V_{12H}$	$V_{41H}$	$V_{23H}$	$V_{34H}$
Sector VI	$V_{23H}$	$V_1$	$V_3$	$V_{41H}$

TABLE V IMPLEMENTED VECTOR SELECTION TABLE

$c_\phi$	+1	+1	-1	-1
$c_\tau$	+1	-1	+1	-1
Periods $T_s$	1 <sup>st</sup>	2 <sup>nd</sup>	1 <sup>st</sup>	2 <sup>nd</sup>
Sector I	$V_3$	$V_1$	$V_2$	$V_3$
Sector II	$V_3$	$V_4$	$V_2$	$V_3$
Sector III	$V_4$	$V_1$	$V_3$	$V_1$
Sector IV	$V_1$	$V_3$	$V_4$	$V_2$
Sector V	$V_1$	$V_2$	$V_4$	$V_3$
Sector VI	$V_2$	$V_3$	$V_1$	$V_3$

An illustration of the previously described control scenarios is provided in Fig. 6. An extension of the synthesis to the remaining sectors has led to the vector selection table given in Table IV. The inputs ( $c\phi$ ,  $c\tau$ , and  $\theta_s$ ) of the vector selection table should be maintained during  $2T_s$  which yields the implemented vector selection table provided in Table V. It is to be noted that both intrinsic and compounded voltage vectors are involved in sectors I, III, IV, and VI, while in sectors II and V, only the compounded voltage vectors are applied. Thus, one can expect an increase of the switching frequency in sectors II and V, with respect to the one in the remaining sectors. In this scheme, each node with message searches for possible path nodes to copy it

- message. Hence, possible path nodes of a node are considered. Using NSS, each node having message selects its path nodes to provide a sufficient level of end-to-end latency while examining its transmission effort.
- Here, it derives the CSS measure to permit CR-Networks nodes to decide which licensed channels should be used. The aim of CSS is to maximize spectrum utilization with minimum interference to primary system.
- Assume that there are M licensed channels with different bandwidth values and y denotes the bandwidth of channel c. Each CR-Networks node

is also assumed to periodically sense a set of M licensed channels.  $M_i$  denotes the set including  $I_{ds}$  of licensed channels that are periodically sensed by node i. suppose that channel c is periodically sensed by node i in each slot and channel c is idle during the time interval x called channel idle duration.

- Here, it use the product of channel bandwidth y and the channel idle duration x,  $t_c = xy$ , as a metric to examine the channel idleness. Furthermore, failures in the sensing of primary users are assumed to cause the collisions among the transmissions of primary users and CR-Networks nodes.

IV. SIMULATION RESULTS

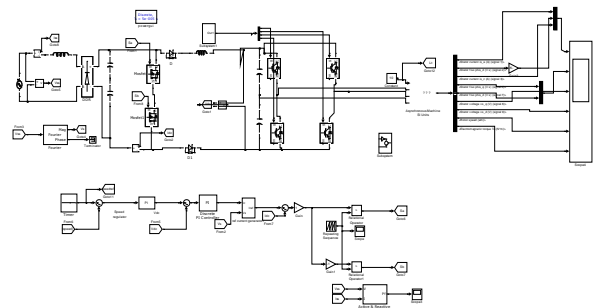


Fig7.simulation digram of DTC Scheme for a Four-Switch Inverter-Fed Induction Motor Emulating the Six-Switch Inverter Operation

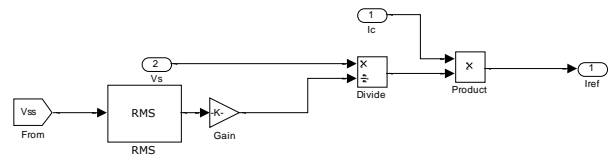


Fig8.Reference Current Wave form Sub system

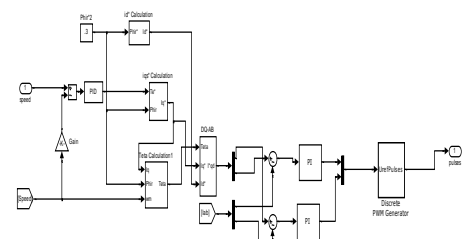


Fig9.Pulse Generator Wave form Sub system

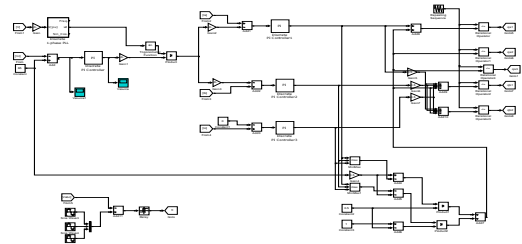


Fig10.Speed Control of induction motor Sub system

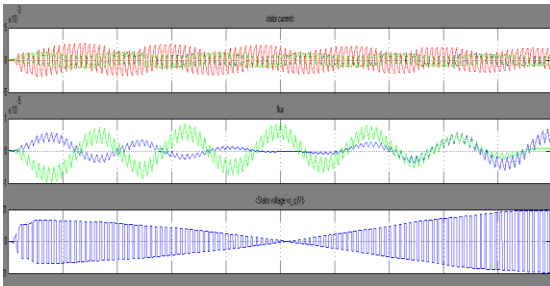


Fig 11(a)

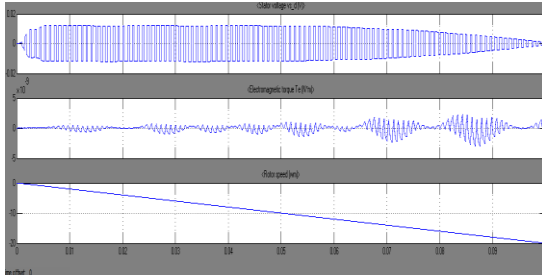


Fig 11(b).

Fig 11..Simulated steady-state variables yielded by the introduced DTC strategy for a reference speed  $\Omega_m = 50$  rad/s and a load torque  $T_l = 1$  Nm. Legend:(a) stator  $a$ -phase voltage, (b) stator  $c$ -phase voltage, (c) stator phase currents, (d) sector succession described in the  $\alpha\beta$  plane, (e) stator flux amplitude and its reference, (f) electromagnetic torque.

## V. CONCLUSION

This paper dealt with a new DTC strategy based SVM modulation controller dedicated to FSTPI fed IM drives. The proposed DTC strategy is based on the reduce of the operation of the conventional of the SSTPI. This approach has been adopted in the design of the vector selection table which is simply addressed by hysteresis controllers, considering a subdivision of the Clarke plane into six sectors. Simulation results of induction motor steady-state features have revealed the high performance of the introduced DTC strategy with FSTPI as compared with the SSTPI.

## REFERENCES

- 1 K. M. Passino, Y. Zhang and J. Zhu, "Direct torque control of permanent magnet synchronous motor with reduced torque ripple and commutation frequency," *IEEE Trans. Power Electron.*, vol. 26, no. 1, pp. 235–248, Jan. 2011.
- 2 B. El Badsı; B. Bouzidi; A. Masmoudi "DTC Scheme for a Four-Switch InverterFed Induction Motor Emulating the SixSwitch Inverter Operation" *IEEE Transactions on Power Electronics* Year: 2013, Volume: 28, Issue: 7Pages: 3528 – 3538.
- 3 K. Reddy Swathi , P. Anjappa , V.Ramesh" DTC Scheme for a Four-Switch InverterFed Induction Motor Emulating the SixSwitch Inverter Operation" *International Journal of Advanced Research in Electrical, Electronics and Instrumentation Engineering*, Vol. 3, Issue 6, June 2014.
- 4 Y. Zhang, J. Zhu, Z. Zhao, W. Xu, and D. G. Dorrell, "An improved direct torque control for three-level inverter-fed induction motor sensorless drive," *IEEE*

*Trans. Power Electron.*, vol. 27, no. 3, pp. 1502–1513, Mar.2012.

- 5 A. Taheri, A. Rahmati, and S. Kaboli, "Efficiency improvement in DTC of six-phase induction machine by adaptive gradient descent of flux," *IEEE Trans. Power Electron.*, vol. 27, no. 3, pp. 1552–1562, Mar. 2012.
- 6 U. M. Choi, H. G. Jeong, K. B. Lee, and F. Blaabjerg, "Method for detecting an open-switch fault in a grid-connected NPC inverter system," *IEEE Trans. Power Electron.*, vol. 27, no. 6, pp. 2726–2739, Jun.2012.
- 7 M. D. Hennen, M. Niessen, C. Heyers, H. J. Brauer, and R. W. De Doncker, "Development and control of an integrated and distributed inverter for a fault tolerant five-phase switched reluctance traction drive," *IEEE Trans. Power Electron.*, vol. 27, no. 2, pp. 547–554, Feb. 2012.
- 8 R. R. Errabelli and P. Mutschler, "Fault-tolerant voltage source inverter for permanent magnet drives," *IEEE Trans. Power Electron.*, vol. 27, no. 2, pp. 500–508, Feb. 2012.
- 9 Q. T. An, L. Z. Sun, K. Zhao, and L. Sun, "Switching function model based fast-diagnostic method of open-switch faults in inverters without sensors," *IEEE Trans. Power Electron.*, vol. 26, no. 1, pp. 119–126, Jan.2011.
- 10 M. N. Uddin and M. Hafeez, "FLC-based DTC scheme to improve the dynamic performance of an IM drive," *IEEE Trans. Ind. Appl.*, vol. 48, no. 2, pp. 823–831, Mar./Apr. 2012.
- 11 H. Zhu, X. Xiao, and Y. Li, "Torque ripple reduction of the torque predictive control scheme for permanent-magnet synchronous motors," *IEEE Trans. Ind. Electron.*, vol. 59, no. 2, pp. 871–877, Feb. 2012.
- 12 A. B. Jidin, N. R. B. N. Idris, A. H. B. M. Yatim, M. E. Elbuluk, and T. Sutikno, "A wide-speed high torque capability utilizing overmodulation strategy in DTC of induction machines with constant switching frequency controller," *IEEE Trans. Power Electron.*, vol. 27, no. 5, pp. 2566–2575, May 2012.